Solubility of Hydrogen in Heavy *n*-Alkanes: Experiments and SAFT Modeling

L. J. Florusse and C. J. Peters
Laboratory of Applied Thermodynamics and Phase Equilibria, Faculty of Applied Sciences, Delft University of Technology, Julianalaan 136, 2628 BL, Delft, The Netherlands

J. C. Pàmies and Lourdes F. Vega
Dept. d'Enginyeria Química, ETSEQ, Universitat Rovira i Virgili, Avinguda dels Països Catalans, 26, 43007, Tarragona, Spain

H. Meijer
Shell Global Solutions International B.V., 1030 BN, Amsterdam, The Netherlands

New experimental measurements on the solubility of hydrogen in several normal alkanes, ranging from decane and up to hexatetracontane, are presented. Data cover a temperature range from 280 K to 450 K, and pressures up to 16 MPa were applied. Hydrogen solubilities of up to 30 mol % were measured. These mixtures are described through a molecular-based equation of state based on the statistical associating fluid theory (SAFT). In the SAFT approach, all the compounds are modeled as homonuclear chains of united-atom sites interacting through a Lennard-Jones potential. Optimized values for the chain length, Lennard-Jones diameter, and dispersive energy characterize the hydrogen molecule. In the case of n-alkanes, a correlation for these molecular parameters is used. Two additional parameters, independent of the thermodynamic variables, were fitted to the experimental data of a single isopleth for each particular mixture. The agreement between the measured and predicted solubilities is excellent (overall AAD < 1.5%) in all the thermodynamic range, and does not significantly worsen as the molecular weight of the compound increases.

Introduction

Hydrogen is a key compound in the production of fuels for the automotive industry and will acquire much more importance in the future, as the free carbon sources of energy tend to emerge for pollution and environmentally evident reasons. Nowadays, hydrogen is mainly obtained from the catalytic steam reforming of nafta and natural gas, but renewable sources of energy seem to be promising for the near future. In many industrial processes where molecular hydrogen plays an important role, its solubility in different hydrocarbon solutions (such as fuels) is among the major factors required for design and optimal operation of these processes. It is also a key parameter in process models, such as the ones used in hydrogenation and hydrotreatment processes, where hydrogen solubility in selected liquid hydrocarbons is a good estimation of the hydrogen concentration in the liquid phase, a variable that is often related to kinetics.

It is well known that empirical and semiempirical models, like traditional cubic equations of state, have limited predictive capabilities, particularly outside the range where their parameters were fitted. On the contrary, parameters of molecular models based on statistical mechanics, like the statistical associating fluid theory (SAFT), have physical meaning and are independent of the thermodynamic conditions. Another important advantage of using a molecular-based theory vs. simple mean-field approaches, is that one can explicitly consider intramolecular as well as intermolecular interactions among the chain molecules involved. Furthermore,

Correspondence concerning this article should be addressed to L. F. Vega.

Table 1. Molecular Parameters for the Pure Compounds

	m	σ (nm)	ϵ/k_B (K)
H_2	0.4874	0.4244	33.85
n-C_{10}	4.259	0.3983	272.7
n-C_{16}	6.407	0.4015	285.0
n-C_{28}	10.70	0.4041	294.7
n-C_{36}	13.57	0.4049	297.8
n-C_{46}	17.86	0.4056	300.6

the details of the applied intermolecular potential will be reflected in the accuracy of the thermodynamic properties calculated by using the theory.

The goal of this work is to provide a reliable model for the prediction of vapor–liquid equilibria and solubility of hydrogen in n-alkanes. To this end, experimental and theoretical work has been carried out in the following binary hydrogen + n-alkane systems: H_2 + n-C_{10}, H_2 + n-C_{16}, H_2 + n-C_{28}, H_2 + n-C_{36}, and H_2 + n-C_{46}.

Experimental Method

Measurements were performed at the Delft University of Technology, using a Cailletet apparatus. Experimental data cover a temperature region from about 280 K to 450 K, and pressures up to 16 MPa were applied. We measured hydrogen solubilities of up to a mole fraction of 30%.

The Cailletet apparatus operates according to the synthetic method. At any desired temperature, the pressure is varied for a sample of constant overall composition until a phase change is observed visually. A sample of fixed and known composition is confined over mercury in the sealed end of a thick-walled Pyrex glass tube. The open end of the tube is placed in an autoclave and immersed in mercury. Thus, mercury is used for both a sealing and a fluid for transmitting pressure to the sample. The sample is stirred by means of a moving stainless steel ball whose movement is activated by reciprocating magnets. The autoclave is connected to a hydraulic oil system that generates the pressure by means of a screw-type hand pump. The temperature of the sample is kept constant by circulating the thermostat liquid through a glass thermostat jacket that surrounds the glass tube. Further details of the apparatus and experimental procedure can be found elsewhere (Raeissi and Peters, 2001).

SAFT modeling

Following previous work, we model the H_2 and alkanes as homonuclear chainlike molecules, formed by tangentially jointed m Lennard-Jones (LJ) segments of equal diameter σ and the same dispersive energy, ϵ. Each of the segments represents a group of atoms, which is known as the united-atom approach. The number of segments m is allowed to take noninteger values to account for a realistic internuclear distance. The accuracy of this model in conjunction with the soft-SAFT approach has been proven in several works (Blas and Vega, 1998; Pàmies and Vega, 2001, 2002).

The soft-SAFT equation of state (EOS) is a modification of the original SAFT equation proposed by Chapman et al.

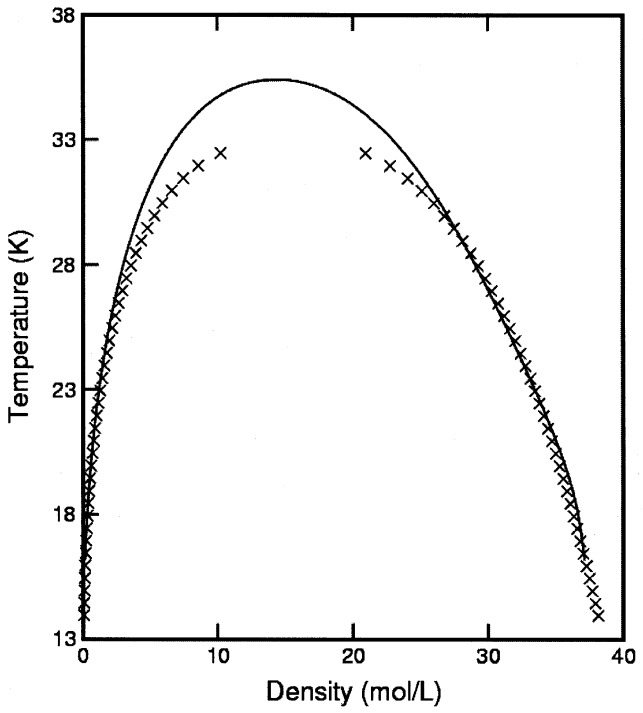

Figure 1. Coexisting saturated densities of pure hydrogen.

Symbols are experimental data from the NIST chemistry Webbook (http://webbook.nist.gov/chemistry) and the line corresponds to predictions of SAFT with optimized parameters for the subcritical region.

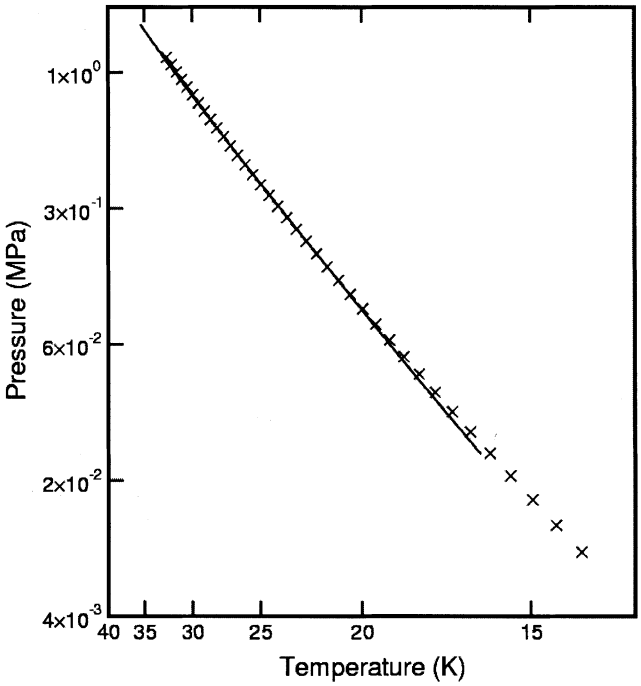

Figure 2. Vapor pressures of pure hydrogen in a log-log plot.

Symbols are experimental data from the NIST chemistry Webbook (http://webbook.nist.gov/chemistry) and the line corresponds to predictions of SAFT with optimized parameters for the subcritical region.

(1989) and Huang and Radosz (1990), which is a first-order perturbation theory (TPT1) based on Wertheim's work. SAFT equations are usually written in terms of the residual Helmholtz free energy, where each term in the equation represents different microscopic contributions to the total free energy of the fluid. Basic expressions concerning this work follow. For a more detailed description of the soft-SAFT EOS, the reader is referred to Pàmies and Vega (2001) and references therein. For an extensive discussion on the development and applications of SAFT equations, see the recent review by Müller and Gubbins (2001).

For nonassociating chain molecules, SAFT equations are usually written as

$$A^{\text{res}} = A^{\text{ref}} + A^{\text{chain}} \tag{1}$$

where A^{res} is the residual Helmholtz energy ($A^{\text{res}} = A^{\text{total}} - A^{\text{ideal}}$). The superscripts *ref* and *chain* refer to the contributions from the monomer and the formation of the chain, respectively.

The original SAFT is based on a hard-spheres reference fluid. In the soft-SAFT EOS, the reference term is a LJ monomer fluid, which accounts both for the repulsive and attractive interactions of the monomers forming the chain.

In the chain and association terms, the original SAFT uses the radial distribution function of hard spheres, while the radial distribution function of a LJ fluid is used in soft-SAFT. The chain contribution for a LJ fluid of tangent spherical segments, obtained through Wertheim's theory, in terms of the chain length, m, and the pair correlation function, g_{LJ}, of LJ monomers, evaluated at the bond length, σ, is

$$A^{\text{chain}} = N_m k_B T \sum_i x_i (1 - m_i) \ln\left(g_{LJ}(\sigma_i) \exp\left[\phi_{LJ}(\sigma_i)/k_B T \right] \right) \tag{2}$$

where N_m is the number of chains, k_B is the Boltzmann constant, T is the temperature, x_i is the mole fraction of component i, and the ϕ_{LJ} is the potential energy.

To calculate the free energy and derived thermodynamic properties of a mixture of LJ fluids, we use the accurate EOS of Johnson et al. (1993), with van der Waals one-fluid mixing rules and the generalized Lorentz-Berthelot combining rules for the crossed interactions

$$\sigma_{ij} = \frac{1}{2} \eta_{ij} (\sigma_{ii} + \sigma_{jj}) \tag{3}$$

$$\epsilon_{ij} = \xi_{ij} (\epsilon_{ii} \epsilon_{jj})^{1/2} \tag{4}$$

The factors η and ξ are the cross-interaction binary parameters.

Table 2. Size Binary Parameter for the Mixtures

	η
H_2 + n-C_{10}	0.8650
H_2 + n-C_{16}	0.8777
H_2 + n-C_{28}	0.8893
H_2 + n-C_{36}	0.8918
H_2 + n-C_{46}	0.8933

Phase-equilibria calculations

Phase-equilibria calculations of binary mixtures with the soft-SAFT equation have been described in detail in previous work (Blas and Vega, 1998). Here we outline only the part needed for the present study.

Molecular parameters for pure H_2 have been calculated by fitting experimental pure hydrogen saturated liquid densities and vapor pressures. Because of the type of model used, the m parameter is allowed to be a fractional number in order to account in some way for the nonsphericity of the molecule. In the next section we will show that this approach is not unrealistic for obtaining excellent results. For n-alkanes, we employ the PV correlation recently published by Pàmies and Vega (2001). All values are given in Table 1. The PV correlation comes from the optimized parameters for the first eight members of the series, and it has been proven to provide very accurate results for vapor–liquid properties of pure heavy n-alkanes and their mixtures (Pàmies and Vega, 2001).

Figures 1 and 2 show the coexisting vapor–liquid densities and vapor pressures of pure hydrogen. The circles are experimental data. (NIST Chemistry Webbook. http://webbook.nist.gov/chemistry). The solid line corresponds to predictions from the equation, using the molecular parameters shown in Table 1. As can be observed in Figure 1, the parameters have been optimized for the subcritical region. Although EOSs with a classical formulation can accurately describe the phase behavior of pure fluids and mixtures far from the critical point, they are unable to predict the near-critical region. This problem can also be explained as a difficulty in describing the critical compressibility factor and critical exponents (Chen and Mi, 2001). To overcome this limitation, a crossover treatment has been used recently in several works. See, for exam-

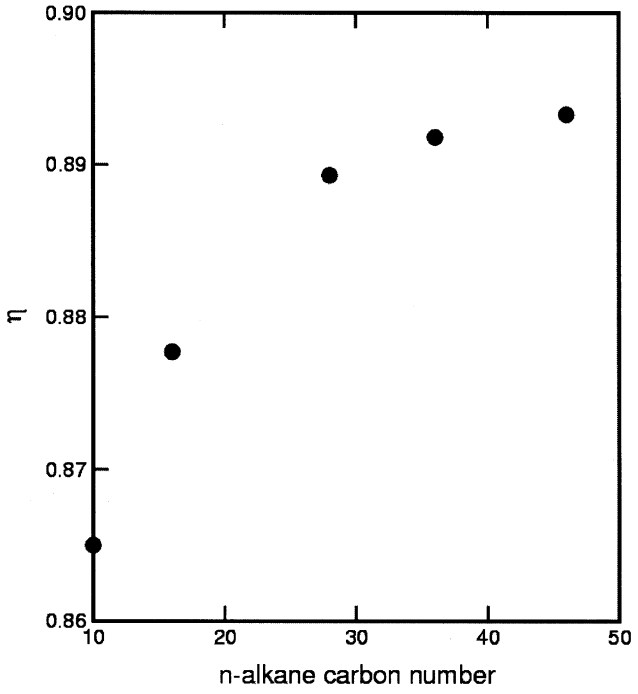

Figure 3. Size binary parameter as a function of the carbon number of the alkane in H_2 + n-alkane mixtures.

ple, the work of Kiselev and Ely (1999). An alternative approach is to rescale the molecular parameters to the critical point (Pàmies and Vega, 2001).

SAFT predictions in Figures 1 and 2 do not cover the temperature region below 16 K, because of the range of validity of the reference EOS for the Lennard-Jones fluid: the temperature range covered by the molecular simulation data that this equation correlates is approximately $0.7 \leq T^* \leq 6.0$. Therefore, although some extrapolation is possible, as shown in these plots, consistent results are not guaranteed. For this reason, experimental data under 23.7 K ($T^* = 0.7$) was not used in the optimization of the parameters for the hydrogen molecule.

Because of the asymmetry of the binary mixtures we are dealing with, the two cross-interaction binary parameters η and ξ should also be fitted to experimental data. One of the main advantages of using such a molecular-based EOS is that parameters should not depend on the thermodynamic conditions. Hence, the procedure we take is to use a *single set* of data, for example, along an isopleth, to adjust the size parameter while maintaining the energy parameter at a constant optimized value along the homologous series. Then we use the optimized values to predict equilibrium properties at any other thermodynamic condition. The fitted values of the cross-interaction size parameter are given in Table 2. The energy parameter was fixed at $5.000 \cdot 10^{-2}$. This number makes the hydrogen–alkane segment cross-interaction energy ϵ_{12} much lower than the interaction energy of the alkane–alkane and hydrogen–hydrogen segments, which is consistent with the low solubilities measured. Figure 3 shows the trend of the size parameter with respect to the carbon number of the normal alkane. This trend is the same as that of the size parameter, σ, of the *n*-alkane homologous series (Pàmies and Vega, 2001), and asymptotically tends to a constant value as

Table 3. Measured Solubility Data for the H_2 (1) + *n*-Decane (2) Mixture*

T (K)	P (MPa)	T (K)	P (MPa)	T (K)	P (MPa)
$x_1 = 0.016$		$x_1 = 0.051$		$x_1 = 0.078$	
283.17	2.568	283.26	8.545	283.21	13.485
283.22	2.573	298.19	7.775	298.13	12.265
298.14	2.343	313.06	7.135	313.08	11.215
298.15	2.348	328.06	6.565	328.02	10.315
313.05	2.163	343.01	6.075	342.98	9.535
313.12	2.158	357.63	5.645	357.56	8.875
328.04	1.993	357.99	5.645	357.94	8.845
342.98	1.843	372.57	5.255	373.06	8.215
357.79	1.723	387.62	4.905	387.97	7.665
357.88	1.718	402.57	4.585	402.85	7.165
372.84	1.608	417.52	4.305	417.74	6.705
387.76	1.508	432.46	4.045	432.62	6.295
402.66	1.418	447.34	3.815	447.66	5.905
417.83	1.343				
432.71	1.283				
447.61	1.238				
$x_1 = 0.031$		$x_1 = 0.056$		$x_1 = 0.088$	
283.22	5.025	283.23	9.463	298.16	14.216
298.13	4.585	298.09	8.613	313.10	12.996
312.96	4.215	313.01	7.893	328.04	11.946
327.92	3.895	328.02	7.273	343.08	11.026
342.91	3.595	343.08	6.713	357.66	10.226
357.74	3.345	357.94	6.243	358.09	10.216
357.87	3.345	373.03	5.793	372.57	9.506
372.79	3.115	387.77	5.413	387.61	8.866
387.76	2.915	403.56	5.033	402.55	8.276
403.03	2.725	418.24	4.733	417.54	7.736
417.94	2.565	433.85	4.443	432.43	7.246
432.65	2.435	447.92	4.203	447.41	6.806
447.53	2.325				
$x_1 = 0.038$		$x_1 = 0.067$			
283.22	6.335	283.21	11.635		
298.10	5.775	298.11	10.575		
313.07	5.295	313.07	9.685		
327.81	4.885	328.07	8.905		
342.73	4.525	343.07	8.235		
357.69	4.205	358.00	7.635		
357.99	4.195	359.18	7.575		
372.79	3.905	373.80	7.055		
387.80	3.645	388.73	6.585		
402.71	3.425	405.35	6.105		
417.69	3.215	419.52	5.735		
432.60	3.035	435.18	5.375		
448.46	2.865	449.63	5.065		

Note: x is the mole fraction.

the length of the chain increases, representing the effective value for the $H_2^- CH_2$ interaction. Additionally, the alkane chain length times η linearly varies with the carbon number, which easily allows us to obtain, with confidence, the η values for other H_2 + *n*-alkane mixtures.

Results and Discussion

We present measurements of the solubility of H_2 in *n*-decane, *n*-hexadecane, *n*-octacosane, *n*-hexatriacontane, and *n*-hexatetracontane, and predictions from the soft-SAFT EOS for this system. Experimental data are summarized in Tables 3–7. We also check the performance of the modified Peng-Robinson (PR) EOS, as found in the Hysys Plant 2.4.1 process-engineering simulator. Several reasons led us to choose this equation for comparison. On the one hand, PR is one of the most used equations in the process industry, and it has been proven to provide very good predictions for alkane binary systems (Pàmies and Vega, 2001, and references therein). On the other hand, we found it very appropriate to use a version embedded in a commercial package, since this is the path engineers usually take in order to use phase-equilibrium data for the design and optimization of chemical processes.

Table 4. Measured Solubility Data for the H_2 (1) + *n*-Hexadecane (2) Mixture

T (K)	*P* (MPa)	*T* (K)	*P* (MPa)	*T* (K)	*P* (MPa)
x_1 = 0.018		x_1 = 0.078		x_1 = 0.109	
298.13	2.266	298.21	10.951	312.97	14.307
313.11	2.071	313.21	9.991	327.81	13.127
328.09	1.921	328.17	9.166	342.75	12.127
343.07	1.781	343.04	8.461	357.64	11.267
357.97	1.656	357.91	7.856	357.86	11.217
358.07	1.656	358.03	7.851	372.78	10.467
372.79	1.551	372.85	7.331	387.71	9.767
387.80	1.451	387.91	6.866	402.62	9.147
403.05	1.361	403.17	6.446	417.66	8.577
418.19	1.286	418.21	6.066	432.54	8.077
432.82	1.216	432.92	5.711	447.34	7.607
448.02	1.151	448.17	5.341		
x_1 = 0.035		x_1 = 0.086		x_1 = 0.113	
298.16	4.600	313.05	10.970	313.04	15.134
313.07	4.205	327.93	10.190	327.96	13.884
328.09	3.870	342.94	9.320	342.96	12.824
343.05	3.590	354.76	8.780	357.60	11.914
357.63	3.345	357.73	8.650	357.98	11.904
357.99	3.345	372.96	8.060	372.67	11.084
373.03	3.115	387.90	7.540	388.00	10.344
387.81	2.920	402.83	7.060	402.83	9.694
402.84	2.745	417.78	6.650	417.71	9.104
417.81	2.580	432.65	6.260	432.75	8.564
432.75	2.435	447.54	5.910	447.59	8.074
447.71	2.300				
x_1 = 0.056		x_1 = 0.091			
313.07	6.893	312.84	11.640		
328.11	6.343	327.87	10.700		
343.03	5.873	342.66	9.930		
357.66	5.473	357.75	9.190		
358.00	5.463	357.81	9.190		
372.64	5.103	372.97	8.550		
387.68	4.773	387.90	7.980		
402.76	4.483	402.78	7.490		
417.72	4.213	417.65	7.040		
432.65	3.973	432.66	6.630		
447.52	3.753	447.52	6.250		
x_1 = 0.073		x_1 = 0.094			
313.07	9.203	313.05	12.153		
328.01	8.463	328.00	11.143		
343.05	7.823	343.02	10.303		
357.94	7.273	357.80	9.563		
357.95	7.263	357.95	9.573		
372.93	6.763	373.18	8.883		
372.93	6.763	388.01	8.303		
387.96	6.333	403.01	7.783		
402.93	5.943	417.90	7.333		
417.85	5.583	432.69	6.923		
432.76	5.263	447.56	6.523		
447.58	4.963				

Note: x is the mole fraction.

Table 5. Measured Solubility Data for the H_2 (1) + *n*-Octacosane (2) Mixture

T (K)	P (MPa)	T (K)	P (MPa)	T (K)	P (MPa)
$x_1 = 0.030$		$x_1 = 0.091$		$x_1 = 0.143$	
342.68	2.245	342.67	7.468	342.60	12.581
357.58	2.085	357.63	6.928	357.52	11.681
372.49	1.955	372.73	6.458	372.45	10.891
387.48	1.835	387.62	6.058	387.50	10.191
402.45	1.735	402.48	5.708	402.45	9.581
417.39	1.635	417.55	5.388	417.43	9.041
432.27	1.545	432.47	5.098	432.39	8.551
447.13	1.465	447.31	4.838	447.32	8.131
$x_1 = 0.054$		$x_1 = 0.106$		$x_1 = 0.178$	
342.68	4.165	342.56	8.613	372.49	14.001
357.70	3.865	357.53	7.973	387.48	13.101
372.79	3.605	372.45	7.453	402.43	12.311
387.80	3.385	387.48	6.983	417.40	11.611
402.52	3.185	402.40	6.563	432.32	10.991
417.46	3.005	417.37	6.193	447.23	10.411
432.39	2.845	432.32	5.863		
447.34	2.705	447.26	5.553		
$x_1 = 0.071$					
342.59	5.841				
357.49	5.421				
372.47	5.061				
372.49	5.071				
387.47	4.751				
402.42	4.461				
417.35	4.221				
432.28	3.981				
432.33	3.981				
447.21	3.771				

Note: x is the mole fraction.

In Figure 4 the symbols represent our primary experimental data (isopleths), which are summarized in Table 3. The symbols in Figure 5 represent the solubility of H_2 in liquid *n*-decane for a number of isotherms, which have been calculated from the primary experimental data, as summarized in Table 3 and depicted in Figure 4. In both Figures 4 and 5, the solid lines are the soft-SAFT predictions using the parameters of Tables 1 and 2. Excellent agreement is obtained, with an absolute averaged deviation (AAD) of about 0.8%. Only about 12.5% of the measurements have been used to fit the cross-interaction parameters, but it is impossible to distinguish which of the isopleths in Figure 4 was chosen. Dot-dashed lines in this figure correspond to predictions using the PR EOS, which are shown for three selected isopleths. This EOS performs equally well as the soft-SAFT EOS, except at low temperatures, where it declines toward lower pressures.

Figures 6 and 7 show experimental data (Tables 4 and 5) and theoretical results for the H_2 + *n*-C_{16} and H_2 + *n*-C_{28} mixtures, respectively. In these figures, the accuracy of the SAFT predictions is similar to that obtained for the lighter alkane (*n*-decane). On the other hand, the performance of

Table 6. Measured Solubility Data for the H_2 (1) + *n*-Hexatriacontane (2) Mixture

T (K)	P (MPa)	T (K)	P (MPa)	T (K)	P (MPa)
$x_1 = 0.033$		$x_1 = 0.097$		$x_1 = 0.169$	
357.62	1.985	357.53	6.188	357.54	11.921
372.53	1.845	372.54	5.778	372.52	11.101
387.54	1.735	387.61	5.418	387.54	10.391
402.52	1.625	402.60	5.098	402.49	9.771
417.50	1.535	417.48	4.818	417.47	9.201
432.46	1.455	432.41	4.558	432.41	8.731
447.43	1.375	447.35	4.328	447.35	8.281
$x_1 = 0.066$		$x_1 = 0.118$		$x_1 = 0.210$	
357.56	4.069	357.60	7.881	372.53	14.341
372.53	3.799	372.53	7.341	387.57	13.421
387.64	3.559	387.58	6.881	402.50	12.621
402.55	3.349	402.53	6.471	417.48	11.901
417.48	3.159	417.49	6.101	432.37	11.261
432.43	2.999	432.41	5.791	447.23	10.681
447.39	2.849	447.36	5.511		

Note: x is the mole fraction.

Table 7. Measured Solubility Data for the H_2 (1) + *n*-Hexatetracontane (2) Mixture

T (K)	P (MPa)	T (K)	P (MPa)	T (K)	P (MPa)
x_1 = 0.065		x_1 = 0.129		x_1 = 0.204	
372.61	3.063	372.59	6.741	372.52	11.811
387.64	2.853	387.55	6.311	387.57	11.041
402.62	2.683	402.51	5.941	402.54	10.391
417.61	2.533	417.51	5.601	417.44	9.801
432.50	2.403	432.37	5.311	432.37	9.271
447.48	2.293	447.32	5.041	447.27	8.811
x_1 = 0.095		x_1 = 0.173		x_1 = 0.257	
372.71	4.623	372.58	9.461	372.57	15.970
387.64	4.333	387.66	8.841	387.61	14.910
402.60	4.083	402.63	8.301	402.69	13.990
417.56	3.853	417.65	7.831	417.73	13.180
432.54	3.653	432.52	7.421	432.58	12.470
447.46	3.463	447.51	7.051	447.50	11.840

*Note: x is the mole fraction.

the PR EOS rapidly deteriorates, and this is more noticeable at the largest mole fraction values of H_2 in the liquid phase.

In Figures 8 and 9 we check the performance of both the soft-SAFT and PR EOS compared to experimental data from Lin et al. (1980), which were measured up to much higher pressures and temperatures than were those we present in this study. The results are a very severe test for the performance of both EOSs in these systems. Data up to 25 MPa and 665 K are used for comparison. No fitting to these data was performed. Cross-interaction parameters for this mixture were optimized using the experimental data of a single isopleth selected from those shown in Figure 6, which are at rather lower pressures and temperatures. Predictions from the SAFT equation are excellent for the liquid phase (Figure 8). Poorer results were expected for the vapor phase (Figure 9), since no information of this phase was used in the optimization of cross-interaction parameters. However, the excellent accuracy of SAFT predictions for the H_2 solubility in the liquid phase, on which this study is focused, is remarkable. PR solubility predictions are much less accurate, although vapor-phase compositions are captured better by PR than by SAFT. We are aware of the somewhat unfair comparison between both EOSs, because, when we used our experimental data, we did not fit any parameter of the PR equation. As

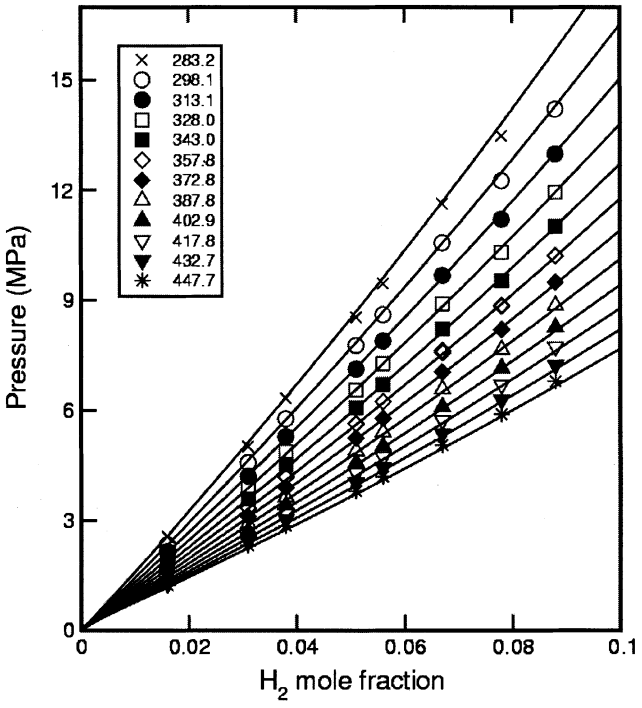

Figure 4. Isopleths of the H_2 + *n*-decane vapor–liquid equilibrium.

Symbols are used for experimental data taken from Table 3, and solid and dot-dashed lines correspond to soft-SAFT and PR predictions, respectively.

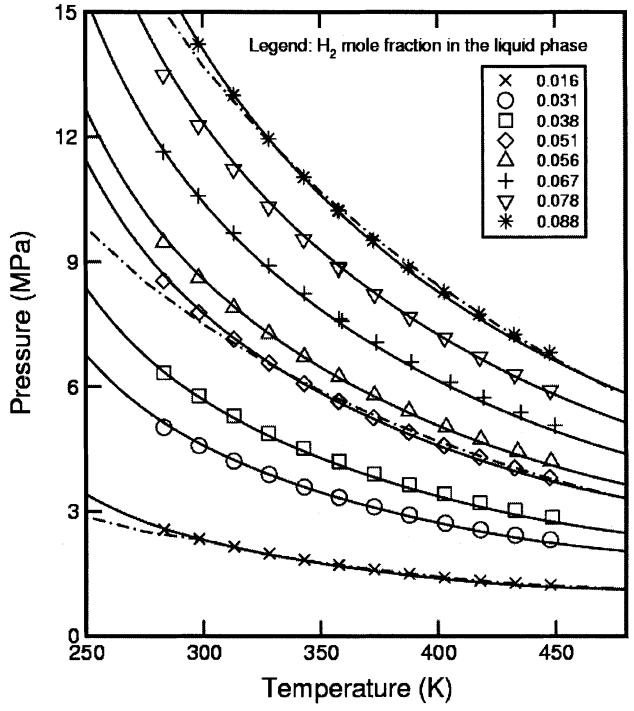

Figure 5. Solubility of hydrogen in *n*-decane, for selected isotherms.

Symbols are interpolated experimental data from Table 3, and lines correspond to soft-SAFT predictions. Temperatures are given in K.

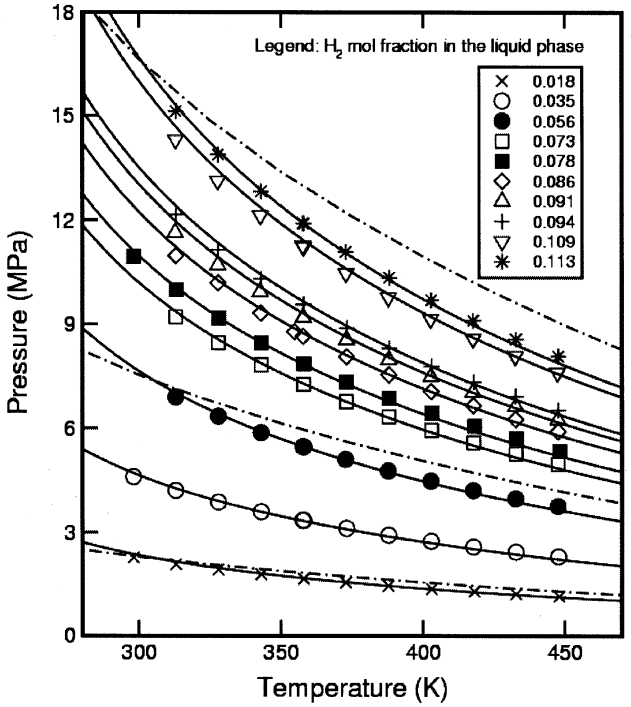

Figure 6. Isopleths of the H_2 + *n*-hexadecane vapor–liquid equilibrium.

Symbols are used for experimental data taken from Table 4, and solid and dot-dashed lines correspond to soft-SAFT and PR predictions, respectively.

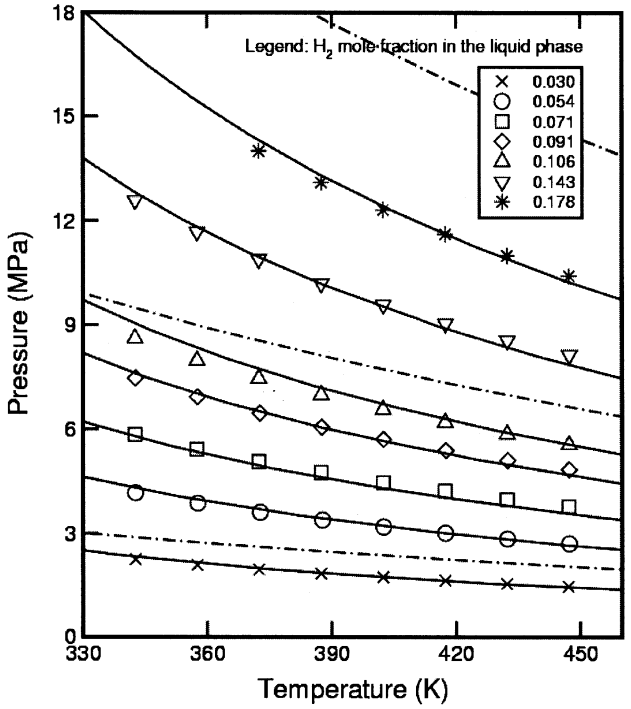

Figure 7. Isopleths of the H_2 + *n*-octacosane vapor–liquid equilibrium.

Symbols are used for experimental data taken from Table 5, and solid and dot-dashed lines correspond to soft-SAFT and PR predictions (at x_1 = 0.030, 0.091, and 0.178), respectively.

mentioned before, our aim is to show the performance of the Hysys modified version of the PR EOS, with all parameters from the Hysys database. It has already been proven (Park et al., 1995) that the fitting of the PR binary interaction parameter to *each* experimental isotherm will provide much better results. But the predictive capability of the EOS is not shown in this way. The performance of the PR equation depends strongly on the α function and the binary interaction parameter used. Although the effect of the binary parameter can be minimized through an optimized temperature-dependent α function (Twu et al., 1995), we believe that to fit parameters depending on temperature is an unavoidable requirement for obtaining accurate predictions using cubic EOSs. On the contrary, the soft-SAFT EOS does not have temperature-dependent parameters, and we only use data of a *single* experimental isopleth for the optimization of the binary interaction parameter of the mixture. In this way, we use SAFT in a fully predictive way at other thermodynamic conditions.

Figures 10 and 11 present experimental data (Tables 6 and 7, respectively), and model predictions for the binary systems H_2 + *n*-C_{36} and H_2 + *n*-C_{46}, respectively. Due to the proximity to the triple point of the *n*-hexatetracontane, no thermodynamically consistent solutions for the SAFT EOS could be obtained below approximately 400 K. These stringent thermodynamic conditions lie far beyond the thermodynamic range of validity of the LJ reference EOS (see the section entitled Phase-Equilibria Calculations). The same reasoning can be used for the H_2 + *n*-C_{36} mixture below approximately 360 K (Figure 10). Nevertheless, accuracies remain as low as for those mixtures with the lower chain-length alka-

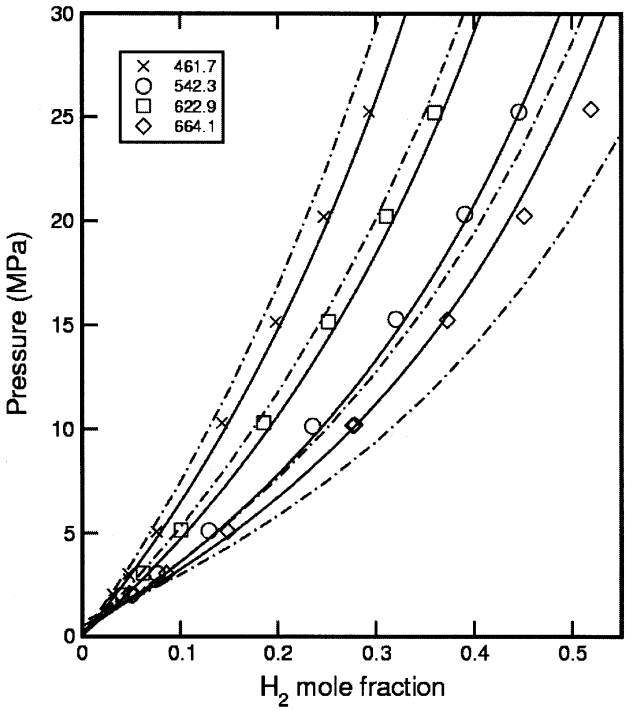

Figure 8. Solubility of H_2 in *n*-hexadecane, for selected isotherms.

Symbols are experimental data taken from Lin et al. (1980), and solid and dot-dashed lines correspond to soft-SAFT and PR predictions, respectively. Temperatures are given in K.

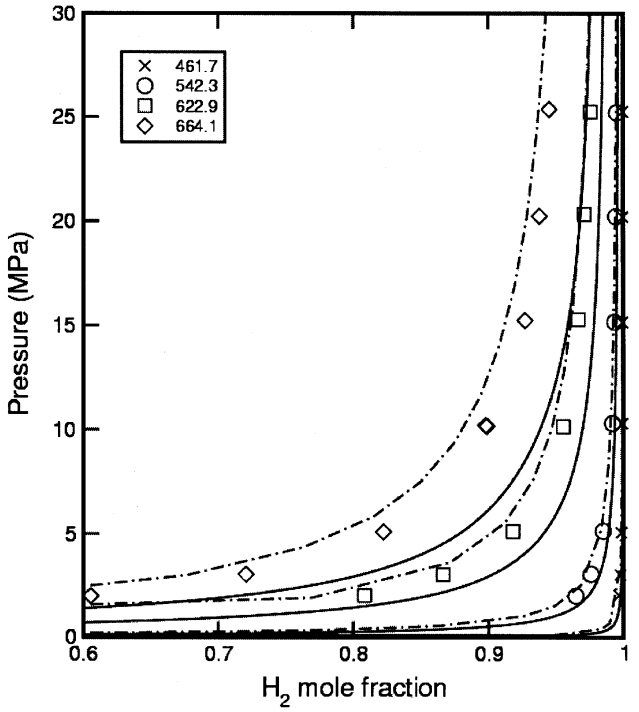

Figure 9. Equilibrium mole fraction of hydrogen in the vapor phase of the H_2 + *n*-hexadecane mixture, for selected isotherms.

Symbols are experimental data taken from Lin et al. (1980) and solid and dot-dashed lines correspond to soft-SAFT and PR predictions, respectively. Temperatures are given in K.

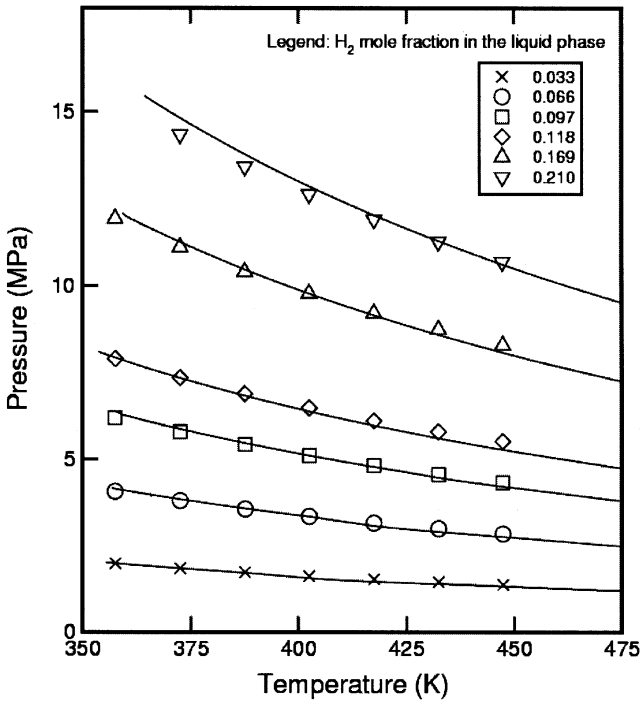

Figure 10. Isopleths of the H_2 + *n*-hexatriacontane vapor–liquid equilibrium.

Symbols are used for experimental data taken from Table 6, and solid lines correspond to soft-SAFT predictions.

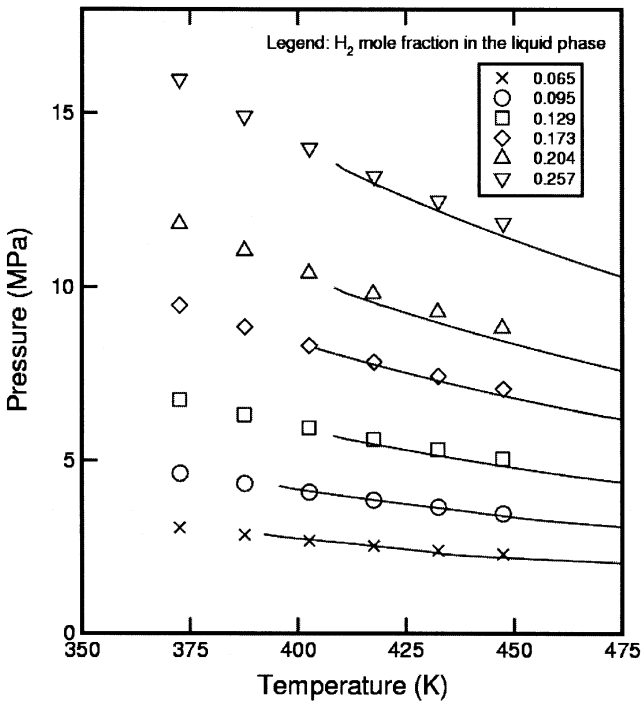

Figure 11. Isopleths of the H_2 + *n*-hexatetracontane vapor–liquid equilibrium.

Symbols are used for experimental data taken from Table 7, and solid lines correspond to soft-SAFT predictions.

nes, except for the highest solubilities of H_2, where deviations can increase up to an AAD of 2.5%. Consequently, the length of the alkane chain does not significantly influence the accuracy of the predictions, at least for the range of chain-length studied here. The overall AAD of soft-SAFT predictions with respect to solubility measurements (Tables 3–7) is less than 1.5%. PR predictions are not included in Figures 10 and 11, since the two heaviest alkanes are not available in the Hysys Plant library.

To summarize, the molecular model, in conjunction with the soft-SAFT theory, provides very reliable results for the solubility of H_2 in *n*-alkane systems in a wide range of pressures and temperatures. Furthermore, the accuracy of the predictions is independent of the thermodynamic conditions and the length of the alkane chain. It is also important to note that, to some extent, the success of the soft-SAFT theory relies on the physical meaning of the molecular parameters (such as segment size, dispersive energy, and chain length). Although their values are effective, their physical meaning is conserved, as we have already seen in Figure 3. As was recently discussed (Pàmies and Vega, 2001), parameters should be optimized by considering the experimental information range needed to later reproduce the thermodynamic features of interest. For H_2 + *n*-alkane mixtures, the experimental data from a single isopleth suffices to provide excellent predictions, provided that molecular parameters have been optimized following a meaningful trend.

Conclusions

Experimental data on the solubility of hydrogen in heavy *n*-alkanes and SAFT modeling of these very asymmetric sys-

tems have been presented. For the five selected mixtures studied (H_2 + n-C_{10}, H_2 + n-C_{16}, H_2 + n-C_{28}, H_2 + n-C_{36}, and H_2 + n-C_{46}), the data covered a temperature range from about 280 K up to 450 K, and pressures up to 16 MPa were applied. The theoretical description is performed using the soft-SAFT equation of state, which describes the fluid systems through a chainlike homonuclear model of Lennard-Jones segments, bonded tangentially to form the chain. Optimized values for the vapor–liquid equilibria of the pure compounds are used to predict the behavior of the mixtures. In addition, the binary size interaction parameter of the generalized Lorentz-Berthelot combining rules was fitted to the experimental data of a single isopleth and used to quantitatively describe the same system in the whole range of experimental conditions, in a fully predictive manner. The overall absolute averaged deviation of SAFT predictions with the experimental data is less than 1.5%. SAFT predictions are excellent over the entire thermodynamic range where data were measured. The accuracy is independent of the thermodynamic variables, and does not get significantly worse as the chain length of the n-alkane increases. Consequently, it is proven that for H_2 + n-alkane mixtures, the soft-SAFT molecular model is able to provide very accurate and reliable results whenever optimized parameters remain meaningful, that is, follow physically meaningful trends.

Acknowledgments

The experimental work of this study was financed by Shell Global Solutions International B.V., Shell Research and Technology Centre, Amsterdam, The Netherlands. Financial support for this work has also been provided by the Spanish Government, under projects PPQ2000-2888-E and PPQ-2001-0671. One of the authors (J.C.P.) acknowledges a predoctoral grant from the Departament d'Universitats, Recerca i Societat de la Informació de la Generalitat de Generalitat de Catalunya.

Literature Cited

Blas, F. J., and L. F. Vega, "Prediction of Binary and Ternary Diagrams Using the Statistical Associating Fluid Theory (SAFT) Equation of State," *Ind. Eng. Chem. Res.*, **37**, 660 (1998).

Chapman, W. G., K. E. Gubbins, G. Jackson, and M. Radosz, "Saft-Equation-of-State Solution Model for Associating Fluids," *Fluid Phase Equilib.*, **52**, 31 (1989).

Chen, J., and J. G. Mi, "Equation of State Extended from SAFT with Improved Results for Non-Polar Fluids Across the Critical Point," *Fluid Phase Equilib.*, **186**, 165 (2001).

Coorens, H. G. A., C. J. Peters, and J. de Swaan Arons, "Phase Equilibria in Binary Mixtures of Propane and Tripalmitin," *Fluid Phase Equilib.*, **40**, 135 (1988).

Huang, S. H., and M. Radosz, "Equation of State for Small, Large, Polydisperse, and Associating Molecules," *Ind. Eng. Chem. Res.*, **29**, 2284 (1990).

Johnson, J. K., J. A. Zollweg, and K. E. Gubbins, "The Lennard-Jones Equation of State Revisited," *Mol. Phys.*, **78**, 591 (1993).

Kiselev, S. B., and J. F. Ely, "Crossover SAFT Equation of State: Application for Normal Alkanes," *Ind. Eng. Chem. Res.*, **38**, 4993 (1999).

Lin, H., H. M. Sebastian, and K. Chao, "Gas-Liquid Equilibrium in Hydrogen + n-Hexadecane and Methane + n-Hexadecane at Elevated Temperatures and Pressures," *J. Chem. Eng. Data*, **25**, 252 (1980).

Müller, E. A., and K. E. Gubbins, "Molecular-Based Equations of State for Associating Fluids: A Review of SAFT and Related Approaches," *Ind. Eng. Chem. Res.*, **40**, 2193 (2001).

Pàmies, J. C., and L. F. Vega, "Vapor-Liquid Equilibria and Critical Behavior of Heavy n-Alkanes Using Transferable Parameters from the Soft-SAFT Equation of State," *Ind. Eng. Chem. Res.*, **40**, 2532 (2001).

Pàmies, J. C., and L. F. Vega, "Critical Properties of Homopolymer Fluids Studied by a Lennard-Jones Statistical Associating Fluid Theory," *Mol. Phys.*, **100**, 2519 (2002).

Park, J., R. L. Robinson, Jr., and K. A. M. Gasem, "Solubilities of Hydrogen in Heavy Normal Paraffins at Temperatures from 323.2 to 423.2 K and Pressures to 17.4 MPa," *J. Chem. Eng. Data*, **40**, 241 (1995).

Peters, C. J., "Phase Behavior of Binary Mixtures of Ethane + n-Eicosane and Statistical Mechanical Treatment of Fluid Phases," Ph.D. Thesis. Delft University of Technology (1986).

Raeissi, S., and C. J. Peters, "Bubble-Point Pressures of the Binary System Carbon Dioxide + Linalool," *J. Supercrit. Fluids*, **20**, 221 (2001).

Twu, C. H., J. E. Coon, A. H. Harvey, and J. R. Cunningham, "An Approach for the Application of a Cubic Equation of State to Hydrogen-Hydrocarbon Systems," *Ind. Eng. Chem. Res.*, **35**, 905 (1996).

Manuscript received Jan. 8, 2003, and revision received Apr. 28, 2003.